

Impact of Friction stir lap welding pin positioning on Microstructure and Fracture behavior of Al-Steel

Shubhavardhan R.N

Department of Mechanical Engineering University of Saskatchewan. Canada

ABSTRACT

Al-steel friction stir lap welding (FSLW) experiments have been conducted to study the effects of welding parameters including tool pin positioning on microstructures formed in the Al-steel interface region, and on joint strength. The joint strength is defined as maximum applied force over the width (F_m/w_s) of the test sample, of the welds. Different tool pin positioning and speed conditions were used in the Al-steel FSLW experiments. Macrostructure of the joints and the fracture surfaces of the tensile shear tests, including examination on crack propagation in mixed stir zone were observed with optical microscope and scanning electron microscope (SEM). It was found that when the tool pin was close to the top surface of the bottom steel piece, intermetallic compounds formed along the interface due to the Al-steel reaction, representing incomplete metallurgical joint. When the tool pin position was lowered to just touch the steel piece, a thin and continuous interface intermetallic compounds layer formed. Signs on growth kinetics have suggested that the thin and continuous intermetallic compounds layer formed could only remain thin ($\leq 3\mu\text{m}$), which could bear a high load during tensile shear testing by deforming and fracturing aluminum alternatively, and the resulting F_m/w_s was high. Similarly when the penetrated to bottom piece steel, F_m/w_s significantly reduced due the brittle fracture being dominant inside the mixed stir zone. It was evident that the tool pin penetration has the strong effect on F_m/w_s during FSLW of Al-steel.

Keywords:-Friction stir lap welding, dissimilar metals, Microstructure, Intermetallic compounds, Fracture behavior.

1. Introduction

Welding of aluminum alloy to steel (Al-to-steel) is very important in many automotive and transportation industries but Al-to-steel fusion welding is generally recognized as highly difficult and challenging [1, 2]. Fusion welding of dissimilar steel to aluminum joints can be obtained using different techniques. Zhang et al. [3] used a modified MIG process, called Cold Metal Transfer (CMT) to join aluminum and zinc coated thin steel sheets with Al-Si alloy filler under argon protection. Sierra et al. [4] joined AA6XXX aluminum alloy to a carbon steel through key-hole laser welding finding solid solutions of aluminum in iron and richer aluminum white solute bands of Fe-Al phases. The same authors compared the integrity and mechanical properties of joints produced by either laser welding or GMAW [5]. Choi et al [6] developed a hybrid technique, based on the combination of resistance spot welding and brazing, to spot joint aluminum and steel for automotive applications. These studies have demonstrated that fusion welding of dissimilar aluminum/steel joints is a challenging task; in fact, the choice of welding parameters and the process window are extremely narrow due to the significant difference in the thermo-mechanical properties of the different base materials. Complex weld pool shapes, segregation, inclusions, porosities and inhomogeneous microstructures are the main factors that severely affect the quality of such weldments [7]. Additionally, the low solubility of Fe in Al results in the formation of extremely brittle intermetallic layers that have a detrimental effect on the mechanical strength of the welded joints [8,9]. For these reasons, friction stir welding could represent an attractive solution to limit the occurrence of the above mentioned defects.

FSW of steels and aluminum alloys can be found in literature. Coelho et al. [10] joined two different grades of high strength steels to AA6181-T4 in a butt joint configuration (an offset was given to the tool towards the aluminum plate side). They found similar resistance for the joints obtained with the two material configurations, with a predominant role of the morphology of the Heat Affected Zone (HAZ) and Thermo Mechanically Affected Zone (TMAZ) of the aluminum plate in respect to steel ones. Ozdemir et al. [11] investigated the effect of rotational speed on the interface properties of friction-welded AISI 304L and steel. They found a correlation between the tensile strength of the joint and joining rotational speed. Dehghani et al. [12] investigated joining aluminum alloy to mild steel, and looked into the effect of various FSW parameters such as traverse speed, plunge depth, tilt angle, and tool pin geometry on the formation of intermetallic compounds (IMCs), tunnel formation, and tensile strength. Watanabe et al. [13] investigated the effect of pin rotation speed and pin offset on the mechanical and microstructural behavior of AA5083 aluminum alloy and SS400 low-carbon steel dissimilar joint.



For FSLW, early investigation by Elrefaey et al. [14] clearly established that tool pin slightly penetrating axially to steel is a condition for a metallurgical joint to be established at Al-steel interface, resulting in a good joint strength. Although detailed quantification was not done in Elrefaey et al.'s study, it is clear from their micrographs that the interface region of welds made with pin penetration is a highly irregular structure of mix layers. This Al-steel interface feature has been commonly observed in the subsequent pin penetrating FSLW studies [15–20] and the region is named mixed stir zone by Coelho et al. [17] in their work on characterizing the microstructures in the zone. Intermetallic layers as thin as 0.2 μm in thickness sandwiched with recrystallized fine α -Fe grains in mixed stir zone are shown, their TEM/EDS analysis (65.6 at.% Al and 33.0 at.% Fe, plus minor elements) may indicate that the thin layers are mainly FeAl_2 . It should be pointed out that assigning the structure of either Fe_2Al_5 or FeAl_3 to mixed stir zone relying on SEM/EDS analysis as in [15, 16, 20] may not be sufficiently reliable due to the analytical spot size being large in SEM/EDS. It may also be viewed uncertain to identify structures based on X-ray diffraction on fracture surfaces where peaks from Fe–Al compounds are low in intensity and peaks may have overlapped, as in [14, 18–19]. A similar study of Wei et al. [21] found, instead, different results. Lap joints, obtained joining 3 mm thick AA1060 and 1 mm thick austenitic stainless steel, were produced with varying tool pin height and welding speed. The major finding of their research was that the use of a cutting pin, i.e. a pin that penetrates into the bottom steel sheets, results in enhanced shear strength due to the presence of saw toothed structures.

Tensile-shear testing of lap welds is a common testing method and the strength can be taken as the maximum load divided by the sample width (F_m/w_s). Kimapong and Watanabe [15] reported F_m/w_s ranging from 280 (2800N/10mm) to 559 N/mm (5591 N/10 mm), for a wide range of FSLW and pin penetrating conditions. The reason is unclear as to why some of their welds displaying severe discontinuity with voids are still high in F_m/w_s (400–500 N/mm). Chen and Nakata's [22] reported $F_m/w_s = 163$ N/mm (3250 N/20 mm) for their non-penetrating FSLW Al-to-steel joints. This is a low F_m/w_s value and from their micrographs, a continuous bond cannot be confirmed. More recently, Movahedi et al. [18, 19] conducted pin penetrating experiments over a range of rotation speed (ω) and defects-free welds were made when the forward speed (v) was lower than a certain value (between 110 and 150 mm/min depending on ω). A feature can be observed from their F_m/w_s data that once a weld was defects free its F_m/w_s was very close to ~ 315 N/mm regardless of whatever the ω was. Zheng, Q et al. [23] claimed Al-steel lap joints with zinc foil as filler metal showed better strength than joints without filler metal but the maximum strength they obtained was 280 N/mm (5600N/20mm) which is reasonable value.

In pin-penetrating FSLW studies [14–16, 19], Fe_2Al_5 , FeAl_3 or both in joint region of welds were suspected to cause F_m/w_s reduction although forming intermetallic layers and thus metallurgical bonding established was also believed to be a condition for a good joint strength. However, Movahedi et al. [19] suggested that a thin interface intermetallic layer up to 2 μm could improve F_m/w_s as crack will then propagate through the mixed stir zone. It should be noted that in their micrograph showing the presence of a $\sim 2\mu\text{m}$ interface layer, there is not a mixed stir zone. It can be viewed that at present how intermetallic compounds affect the fracture behavior of the welds, particularly considering that the mixed stir zone in FSLW Al-steel welds is unique, and affect F_m/w_s are unclear. The main objective of the present work is to evaluate the microstructure evolution and fracture behavior of Al-steel FSLW with respect to various tool pin positions, and effects of the tool pin position dependent interface microstructures on fracture behaviors and on F_m/w_s can be established.

2. Experimental Procedure

FSLW experiments were conducted using a milling machine, mounted with LowStirTM unit in the milling machine for monitoring down force (F_z) as shown in Fig 1. As indicated in Fig. 2, the top plate was 6-mm thick aluminum 6060-T5 alloy and the bottom plate was 2.5-mm thick mild steel. The use of the sufficiently thick top plate was to prevent fracturing in heat affect zones and to instead cause fracture along the interface region during mechanical testing. Before each experiment, the steel plate was wire brushed to remove the surface oxide. FS tools were made using heat treated tool steel (H13), in common with that used in the cited studies [14–16, 18, 19, 22]. The diameter of the shoulder was 18 mm and the threaded pin outside diameter was 6 mm. Tool tilt angle was 2.5 degrees.

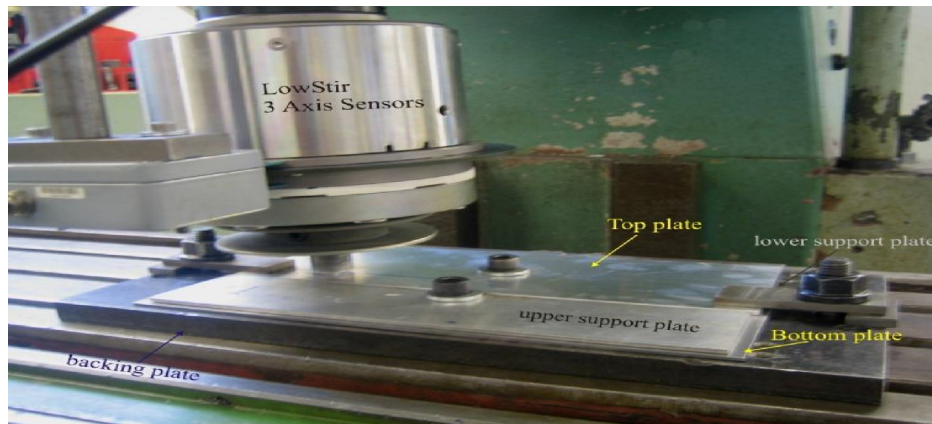


Fig. 1 A milling machine, mounted with LowStir™ used for Al-steel FSLW experiments

A major series of experiments were conducted with $v = 60$ mm/min and $\omega = 800$ rpm, but $\omega = 1200$ rpm was also used for comparison. Various pin positions, expressed as D_p (distance of penetration) in Fig. 2, were used. To ascertain D_p , the tool was first lowered to touch the surface of the top plate and the vertical control handle of the machine was assigned zero. Then, the rotating tool was plunged for the required depth. D_p values were aimed at, -0.4 , 0 and 0.4 mm. Temperature was measured using twisted K type thermocouple wires (0.30 mm in diameter) placed between the lapping surfaces through a narrow groove machined in the bottom plate. The thermocouple junction was placed in a location that the mid of the stir zone bottom passed in each experiment. Thermal conducting paste was applied around the junction tip for a good thermal contact.

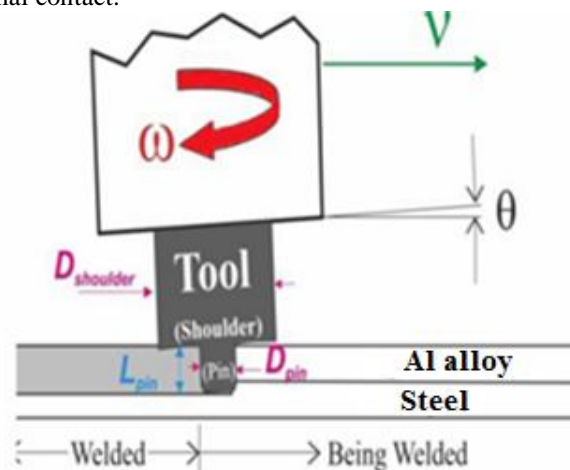


Fig. 2 Schematic illustrations of friction stir lap welding (FSLW) of Al-to-steel with the pin having penetrated to steel

When a FSLW experiment carried out for the weld made with $D_p \approx 0$ mm, the pin was axially located to have just touched the top surface of the bottom plate without penetrating. Figure 3 illustrates the sequence of this experiment. In this figure, F_z values before ~ 115 s correspond to the manual plunging and careful positioning. After the tool started moving forward, F_z increased but later at ~ 160 s the rate of increase became very low, indicating a close to stable condition. The tool was lowered slightly at ~ 240 s to cause an increase in F_z which was not stable indicating the pin bottom having penetrated to steel. This is to make certain the welded section just before this tool pin lowering was in a condition that $D_p \approx 0$. F_z decreased and became stable, meaning touching the top surface of bottom steel plate, when the pin was approaching the mid location of the plate. A likely explanation for this is a slight uneven clamping/bolting (through the hole) thus lowering slightly the steel site in the mid location of the plate although a slight wear of the pin bottom was also possible. In a later part of this welding experiment, at ~ 390 s, the tool was again manually lowered to ascertain a penetration of the pin to steel. After FSLW experiments, samples were taken for tensile-shear testing and for metallography. Examples were taken from welded plates but the initial 20 mm in length and also 20 mm in length in mid location of the plates (along the weld) were excluded from sampling. The samples were taken in Location 1 (Fig. 3) for $D_p \approx 0$ and in Location 2 for $D_p = 0.4$. Tensile-shear test samples and supporting pieces were 16-mm wide. Details of gripping a sample for testing, which is commonly used for testing lap joints, have been explained. Samples were tested at a constant crosshead displacement rate of 3 mm/min using a 50 KN Tinius Olsen tensile machine. A 50-

mm extensometer was attached to the sample during testing. Metallographic samples were mounted and polished, and some samples were etched using modified Keller’s reagent. Microstructure examination was conducted using a Hitachi SU-70 FE SEM with a Thermo Scientific NSS EDS system.

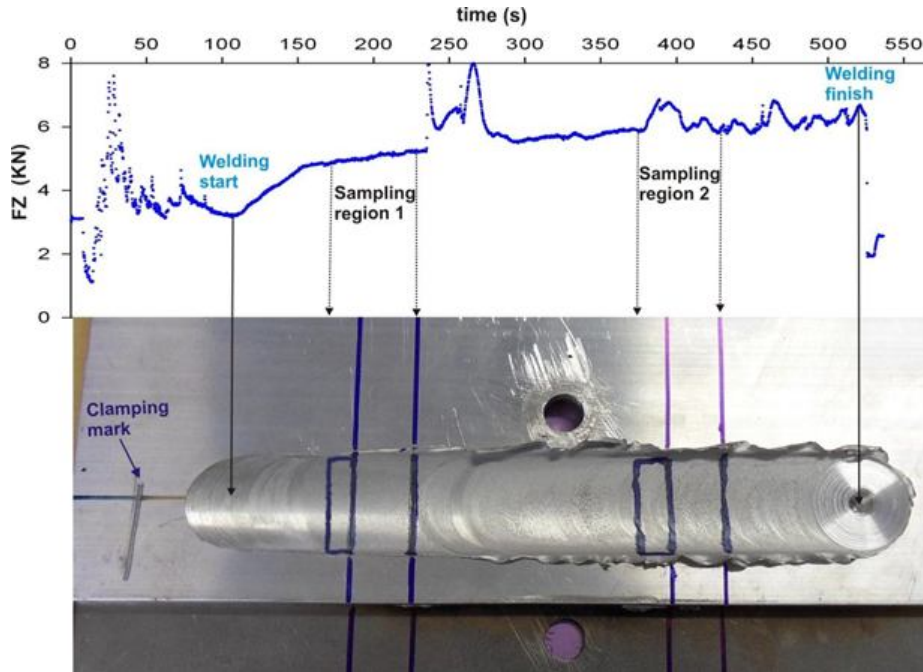
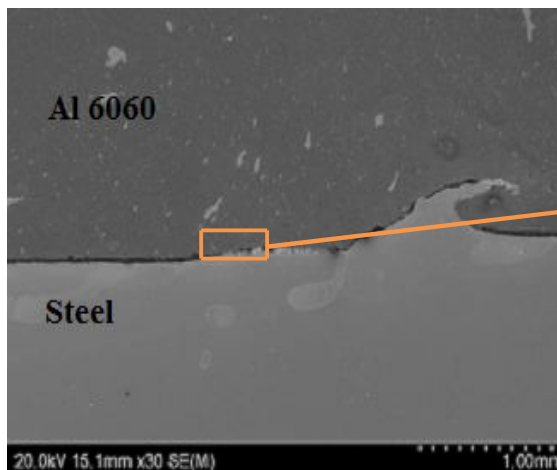


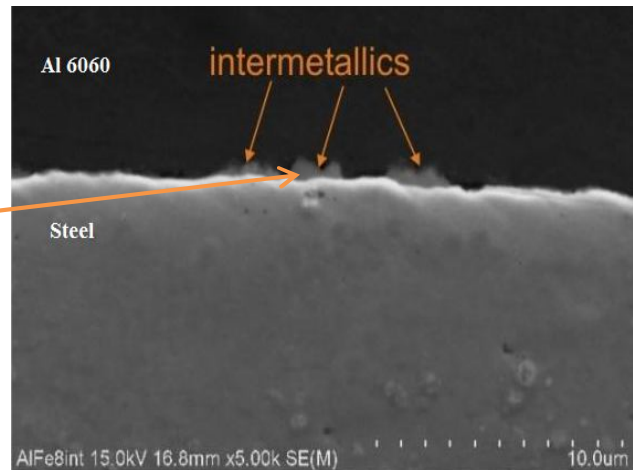
Fig. 3 An Al-Steel FSL Weld made using $\omega=800$ rpm and $v=60$ mm/min with Fz – time curve, location of sampling region 1 and 2 is indicated.

3. Results and discussion

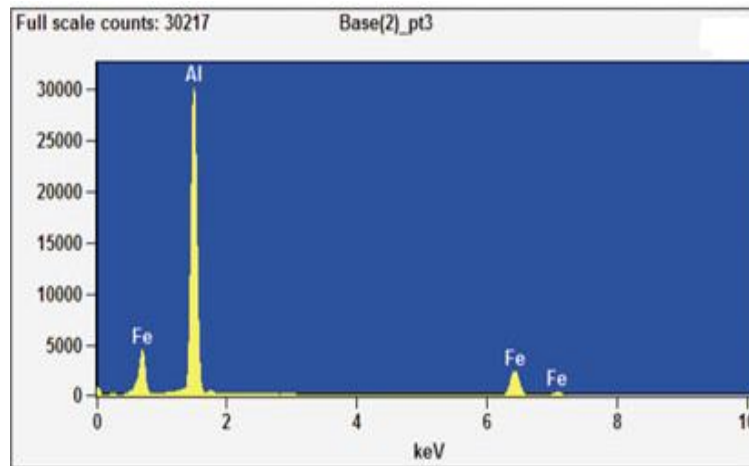
Typical Al-steel interfaces of the welds made using $D_p = -0.4$ mm is shown by SEM micrograph in Fig. 4a. In the sample of the weld made with $D_p = -0.4$ mm, with the higher magnification as shown in Fig. 4b, small ‘intermetallics’ can be observed along the interface, which has not ensured a continuous intermetallic layer, suggesting a non-continuous metallurgical bond. An EDS spectrum from a point analysis on an intermetallic compounds is shown in Fig. 4c and there is not an oxygen peak suggesting that these outbursts are not oxides. Rather they should be Fe–Al intermetallic compounds. The same form of intermetallic compounds at the interface resulting from the early stage of interfacial intermetallic growth in solid Al-steel couples has commonly been observed [24]. As shown in Fig. 4c, many discontinuous intermetallic compounds are seen close to $1\mu\text{m}$ or slightly larger. Thus, it may be suggested that if intermetallic compounds are sufficiently dense to form a continued layer the layer should have a thickness over $1\mu\text{m}$.



(a)



(b)



(c)

Fig. 4 Interface microstructure shown by SEM micrographs taken in welds made with a $D_p = -0.4$ mm, (b) higher magnification of figure (a) displaying intermetallic compounds, (c) EDS spectrum from a point analysis on an intermetallic compounds.

For the weld made for $D_p \approx 0$ mm represents a slight zone with a width significantly smaller than the pin diameter. This zone consists of irregular laminates of fine recrystallized α -Fe grains, thin and continuous Fe–Al intermetallic layers and is the same which has been observed in other authors [14–16, 17–20] on Al–steel welds made using FSLW, as has already been explained in Introduction. At the interface between the mixed stir zone and the top Al stir zone, as shown in Fig. 5a, there is an intermetallic layer with a thickness at $\sim 2 \mu\text{m}$. This interface layer became slightly thicker (just under $3 \mu\text{m}$), as is clear in Fig. 5b, when a considerably higher ω value (1200 rpm compared to 800 rpm) was used during FSLW. The use of a considerably higher ω value, thus significantly higher stir zone temperatures as shown in Fig. 6, allowed the diffusional growth of the interface intermetallic layer to a slightly greater thickness.

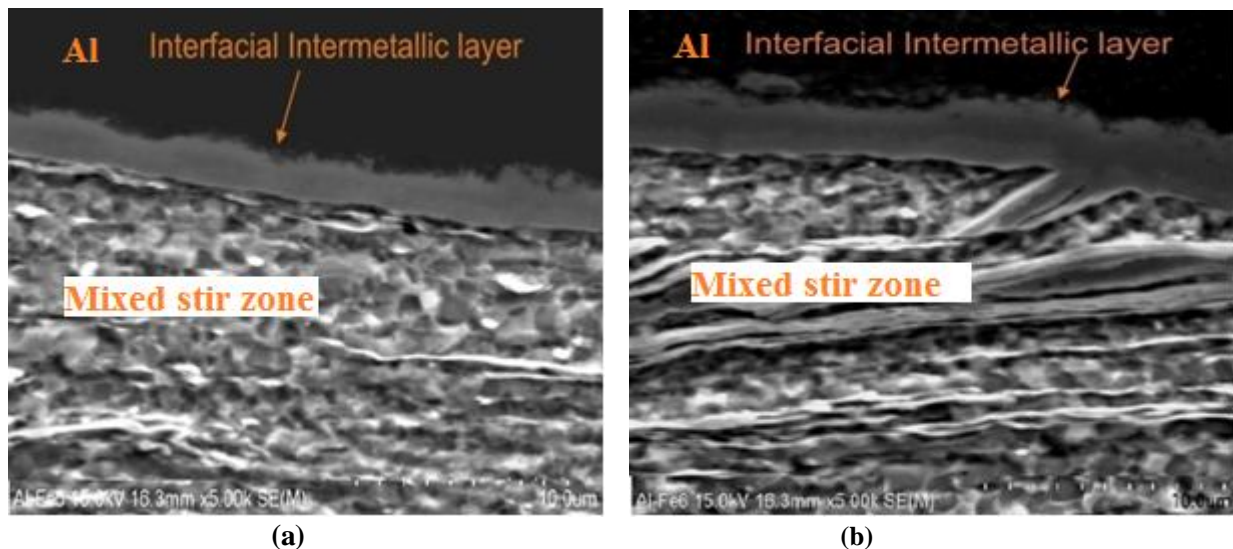


Fig. 5 Microstructures in the interface regions of FSL welds made using $D_p \approx 0$ mm, $v = 60$ mm/min, (a) $\omega = 800$ rpm and (b) $\omega = 1200$ rpm

Microstructures of interface regions for Location 1 ($D_p \approx 0$) and Location 2 ($D_p = 0.4$ mm) in the further experimentare shown in Fig. 7. The top optical micrograph confirms that there was little pin penetration in Location 1. Yet, a rather continued interface intermetallic layer (up to $3 \mu\text{m}$ in thickness) is observed, as shown in the high magnification SEM micrograph. The average composition from a number of EDS point analyses was ~ 70 at.% Al and 30 at.% Fe, thus it cannot be certain if the phase is FeAl_2 or Fe_2Al_5 . Coelho et al. [17] pointed out that structural analysis of the thin interface layer next to Al in FS Al–steel welds is very challenging and their TEM pattern suggests Fe_2Al_5 , which is

orthorhombic. Differing from Location 1, as shown in Fig. 7b, a sufficient pin penetration in Location 2 of the weld made in the further experiment has resulted in forming a mixed stir zone, which is significantly larger than the one made using $D_p \approx 0$ mm as shown in Fig. 5a.

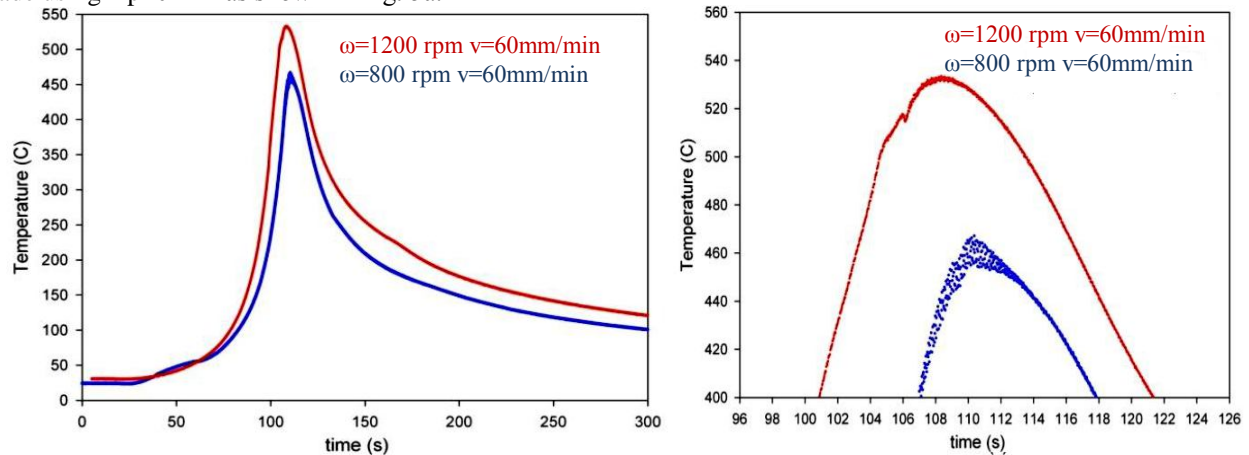


Fig. 6 (a) Measured temperatures at the Al-steel interface region during FSLW, for the welds made using $D_p \approx 0$ mm and ω and v as indicated (b) enlarged view of temperature readings for temperatures > 400 °C

It is thus clear that a pin penetration ($D_p = 0.4$ mm) must result in a mixed stir zone. This zone may be regarded as a simple mechanical consequence of pin penetration. As has also been presented in Fig. 5 and discussed, there is a continued intermetallic layer between the mixed stir zone and Al top plate. The mixed stir zone must decrease in size when D_p decreases and disappears when D_p reaches zero. However, when $D_p \approx 0$, the thin and continued interface intermetallic layer can remain, but in this case this layer is between Al and steel, as the mixed stir zone has disappeared. Further decreasing D_p (< 0) provides a less favorable condition for intermetallic formation and growth, and thus the intermetallic compounds become discontinued along the interface. As D_p decreases further, reaction between Al and steel can no longer take place and thus no metallurgical bond has formed. Once intermetallic compounds become continued as a layer at the interface, the growth rate of the layer must be very low. As already described, for a constant v value ($= 60$ mm/min), an increase of ω from 800 to 1200 rpm resulted in a significant increase in stir zone temperatures (Fig. 6). Temperature should normally have a strong effect on the rate of diffusional growth of the interface intermetallic layer. Yet, as has already been pointed out and is clear in Fig. 5, the layer has only thickened to $\sim 3 \mu\text{m}$ from $\sim 2 \mu\text{m}$. A further FSLW experiment is carried out for the condition of a high rotation speed at $\omega = 1200$ rpm and very low forward speed at $v = 20$ mm/min is a very high heat input condition for friction stir. Yet, very slow growth of the interface intermetallic layer can be noticed, and the interface intermetallic layer could only grow to a maximum $3 \mu\text{m}$, as is shown in Fig. 7.

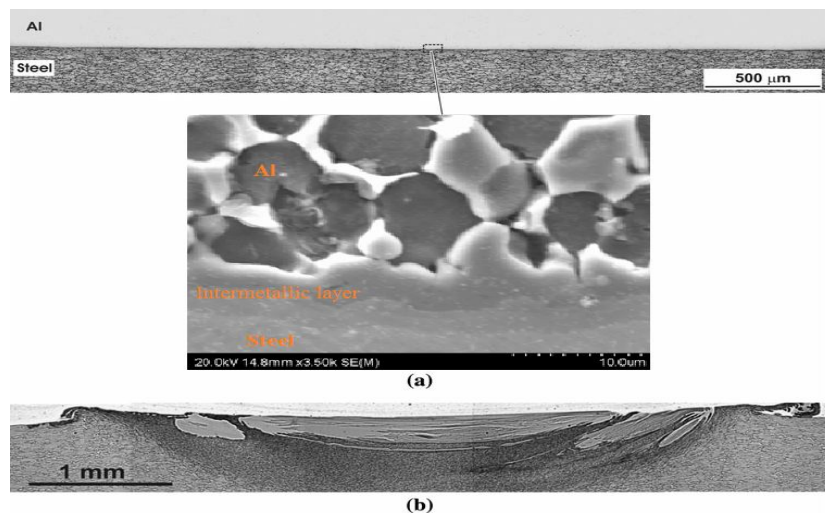


Fig. 7 Interface microstructures of the weld made using $\omega = 1200$ rpm $v = 20$ mm/min (further experiment), a sample taken in Location 1—optical micrograph (top) and SEM micrograph (bottom) taken in location as indicated, b sample taken in Location 2.

The very slow growth rate of Fe–Al interface layer in solid state may be explained by Naoi and Kajihara’s [24] diffusion experiments. They determined the growth constant, k , for relating the square of layer thickness to time for the growth of Fe–Al interface layer to be 0.0034 and 0.0016 $\mu\text{m}^2/\text{s}$, respectively, for 600 and 550 $^\circ\text{C}$. Then, at a thickness of 2 μm , the growth of 1 μm requires 1472 s at 600 $^\circ\text{C}$ and 3125s at 550 $^\circ\text{C}$. Considerably higher k values were obtained based on experiments using Fe–Al friction stirred samples by Springer et al. [25]. If their k value (0.0586 $\mu\text{m}^2/\text{s}$) for 600 $^\circ\text{C}$ is used, 86 s may be required for the growth from 2 to 3 μm at 600 $^\circ\text{C}$. This is still a very slow growth. Peak temperature (Fig. 6) is 538 $^\circ\text{C}$ when $\omega = 1200$ rpm and $v = 60$ mm/min. Temperature measurement during the further experiment ($\omega = 1200$ rpm and $v = 20$ mm/min which is a very high heat input condition) has shown that the peak has broadened considerably (~ 90 s for $T > 400$ $^\circ\text{C}$), but the peak temperature has only increased slightly to 545 $^\circ\text{C}$, as shown in Fig. 8. That the growth constant is known to be very low in this thermal condition is consistent with the observation on the interface intermetallic layer that did not grow beyond 3 μm even in the very high heat input FSLW condition. It should be noted that the peak temperatures detected are significantly lower than the solidus of the alloy which is ~ 610 $^\circ\text{C}$ and thus there is no incipient melting during FSLW.

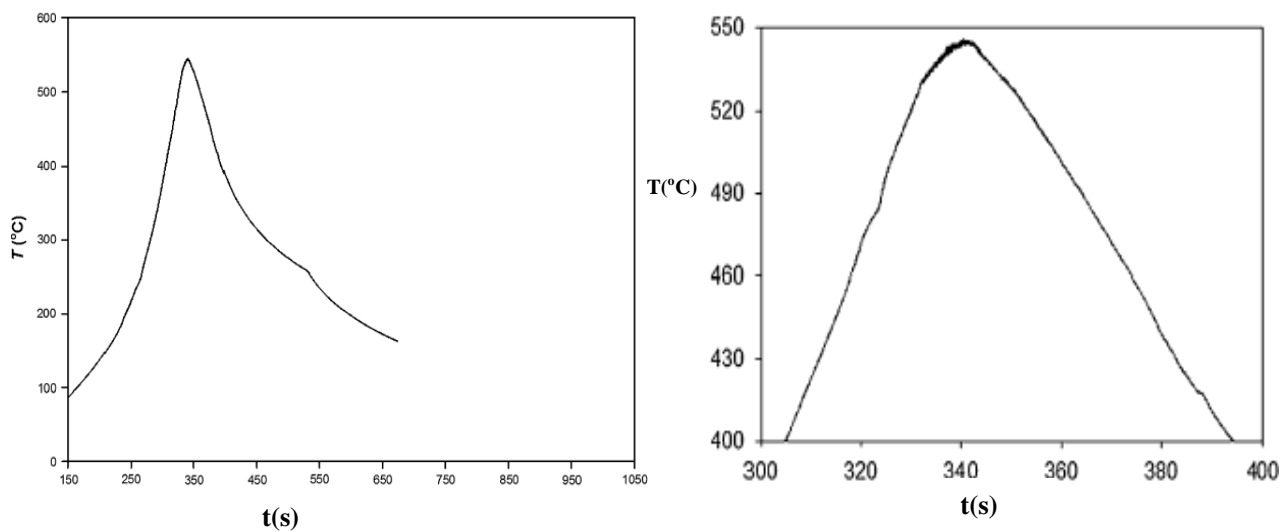


Fig. 8 Temperature history at Al-steel interface region during FSLW for weld made in the further experiment ($\omega = 1200$ rpm and $v = 20$ mm/min)

In Fig. 9a, F_m/w_s data of welds made using the various FSLW conditions are plotted as a function of D_p . The weld showed little strength when $D_p = -0.4$ mm. This is consistent with the observation that, as shown in Fig. 4a, little metallurgical reaction has taken place for the Al top plate to weld on the bottom steel piece due to the presence of intermetallic outbursts (Fig. 4b, 4c), and thus some strength ($F_m/w_s = 130 \pm 10$ N/mm) has developed. For $D_p \approx 0.4$ mm (pin penetration into steel plate), $\omega = 800$ rpm and $\omega = 1200$ rpm were used. This large difference in ω , as has been demonstrated in Fig. 6, resulted in significant differences in peak temperature and in the amount of time at high temperatures of the stir zones. Despite this, F_m/w_s only differed slightly: $F_m/w_s = 307 \pm 15$ N/mm for $\omega = 800$ rpm and $F_m/w_s = 317 \pm 23$ N/mm for $\omega = 1200$ rpm. For the same D_p , but different ω (and/or v), the size of the mixed stir zone should be approximately the same, as the size should largely be a mechanical consequence of how deep the pin penetrates. For the same D_p , but different ω , (and/or v), however, a-Fe grain sizes and the thicknesses of the intermetallic layers inside the mixed stir zone should differ due to the differences in the degree of mechanical mixing/stirring and in thermal history. These mechanical, thermal and thus metallurgical differences did not have a large effect on interface F_m/w_s and $(\Delta F_m/w_s)/(F_m/w_s) \approx 10/307 \approx 3\%$.

Figure 9 shows selected tensile-shear curves. Before discussing the behaviors of the samples from these curves, the strain measurement should be commented on first. Unlike traditional tensile testing where the sample is elongated axially, in a tensile-shear test, the extension is slightly axially off and there is a degree of local rotation during testing if sufficient plasticity of the sample allows. Thus, the axial strain measurement by the extensometer is slightly distorted due to the slightly local twisting/bending. Furthermore, particularly in the initial stage of elongation (largely within the linear range), the extension values measured by the extensometer were slightly unstable. Thus, determined strain values are not highly accurate but the use of them should be adequate for indicating plasticity.

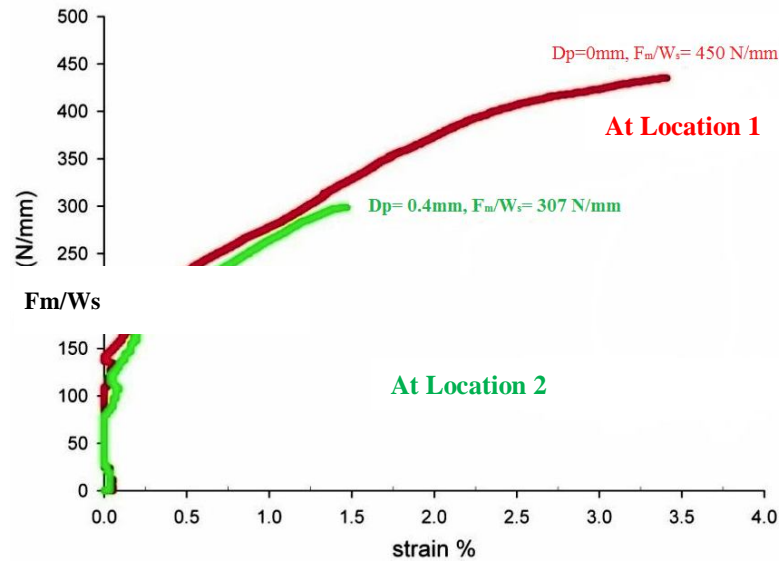


Fig. 9 Tensile-shear testing data of welds made using $\omega=800\text{rpm}$, $v=60\text{mm/min}$; $D_p \approx 0\text{mm}$ and $D_p=0\text{-}4\text{mm}$. (refer Fig 3 for Location 1 & 2)

In the figure 9, from the major series of experiments ($\omega = 800 \text{ rpm}$ and $v = 60 \text{ mm/min}$), and $D_p = -0.4 \text{ mm}$ (non-penetrating) the low fracture load (130 N/mm, which is not shown in the figure 9) without an appreciable amount of plastic deformation. On the other hand, the sample of $D_p= 0.4\text{mm}$ mm fractured at a considerably higher load (307 N/mm) with a significant amount of plastic deformation. There is a significant amount of fracture energy (E_f), represented by the area under the curve, for the pin-penetrating sample and E_f for the non-penetrating sample is basically zero. It can thus be suggested that $F_m/w_s \approx 307 \text{ N/mm}$ is a reasonably good strength value. In comparison, as has already been pointed out, Movahedi et al. [18, 19] conducted a large series of pin penetrating FSLW Al-to-steel experiments and once a weld was defects (voids) free F_m/w_s was very close to the maximum F_m/w_s value which was $\sim 315 \text{ N/mm}$, although this feature was not particularly noted and the physical reason was thus not provided in their study. The sizes of tool shoulder and pin, the shape of pin, the thicknesses of the top and bottom plates, and the tensile-shear sample size used in the present work are, however, all different from those used by Movahedi et al.

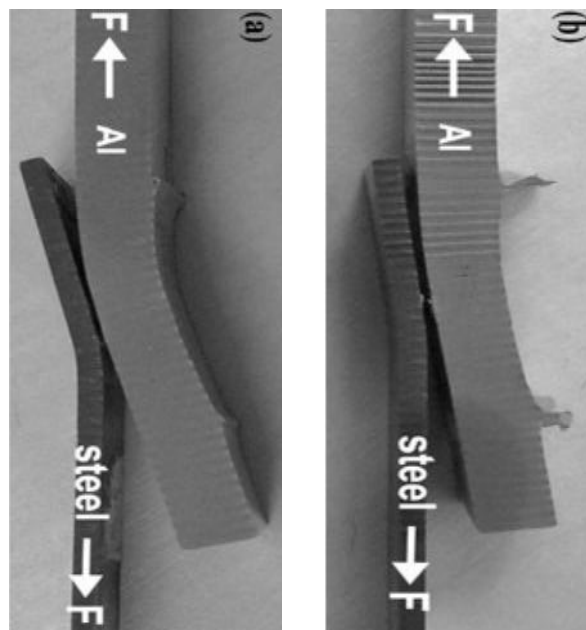


Fig.10 Images of tensile-shear tested samples, (a) Location 1 sample showing significant local bending and (b) Location 2 sample showing only limited local bending. Locations referring to Fig. 3

We now discuss the sample taken in Location 1 ($D_p \approx 0$) of the weld plate made with $\omega = 800$ rpm, $v = 60$ mm/min, which has been explained, is a condition for a continued layer to have formed along the interface. As shown in Fig. 9, F_m/w_s of this zero D_p sample is 450 N/mm and is considerably higher than the F_m/w_s values of all non-zero D_p samples. The overall effect of D_p on F_m/w_s can now be discussed. As shown in Fig. 9, on one side, F_m/w_s increases sharply when the interface intermetallic compounds layer become thin and continued (Fig. 7a) from being discontinued (Fig. 4). On the other side, once the pin penetrates and a mixed stir zone forms, F_m/w_s decreases to ≤ 310 N/mm and is not significantly affected by D_p , ω or v although this discussion only limited for small D_p values. Tensile-shear test curves for samples taken in Locations 1 and 2 are also provided in Fig. 9. The area under the curve (E_f) of Location 1 sample is considerably higher than that of Location 2 sample.

Images of the tested samples from the weld plate made in the further experiment are presented in Fig. 10. The high amount of deformation as shown by the tensile-shear curve in Fig. 9 for Location 1 sample is consistent with that shown in the top image of the tested sample in Fig. 10a which shows that, before the sample fractured, a high amount of deformation in and around the weld region has resulted in a significant local bending. The large deformation is accompanied by a corresponding amount of work hardening, as is indicative in the tensile-shear curve in Fig. 9, and thus by a high F_m/w_s value (450 N/mm). On the other hand, as is clear by comparing the image in Fig. 10a to that in Fig. 10b, the amount of deformation/bending is low in Location 2 sample. This is also agreeable to what are indicated in the tensile-shear curves in Fig. 9, as already explained. Respective SEM micrographs are presented in Fig. 11. In Location 1 sample, as shown in Fig. 11a, ductile fracture is dominant with plastic (shear) deformation preceding failure in aluminum adjacent to and on top of the intermetallic layer. This ductile deformation is consistent with the tensile-shear curve shown in Fig. 9 displaying high fracture strain and energy values, and thus also is consistent with the image in Fig. 10a showing a large amount of local bending.

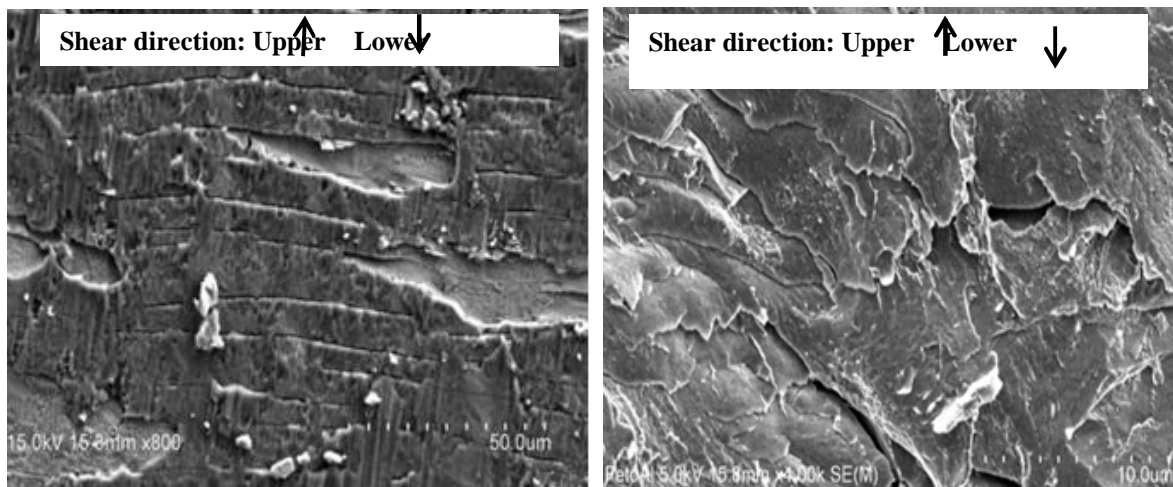


Fig. 11 SEM Micrographs of tensile-shear tested samples in (a) Location 1 displaying heavily deformed ductile fracture of the intermetallic layer and (b) Location 2 displaying brittle fracture of the intermetallic layer

The cracks seen in Fig. 11a are through thickness cracks in the intermetallic layer and perpendicular to the shear direction, having contributed little to the shear deformation and cracking (in Al) processes. On the other hand, a significant portion of the fracture surface of Location 2 sample, as shown in Fig. 11b, has displayed brittle failure feature. It is likely that cracking has propagated along (parallel to) the thin intermetallic pieces/layers in the mixed stir zone during testing. This brittle nature of fracture surface is also consistent with the tensile-shear curve in Fig. 9 showing lower fracture strain and energy values and thus also is consistent with the image in Fig. 10b showing only a very limited amount of local bending. For clarifying further the comparatively brittle nature of pin penetrating welds, a Location 2 sample was tested to 265 N/mm ($\sim 90\%$ of F_m/w_s) and the test was stopped before and without final fracture for the fracture path to be observed in the mixed stir zone. SEM micrographs showing part of the mixed stir zone of the tested sample with a major crack well developed are given in Fig. 12. The crack has propagated quite intensively and deep inside the mixed stir zone along either the thin intermetallic layers or the interface between a thin intermetallic layer and a-Fe grains. This is consistent with the observed brittle fracture as observed in the fracture surface shown in Fig. 11b.

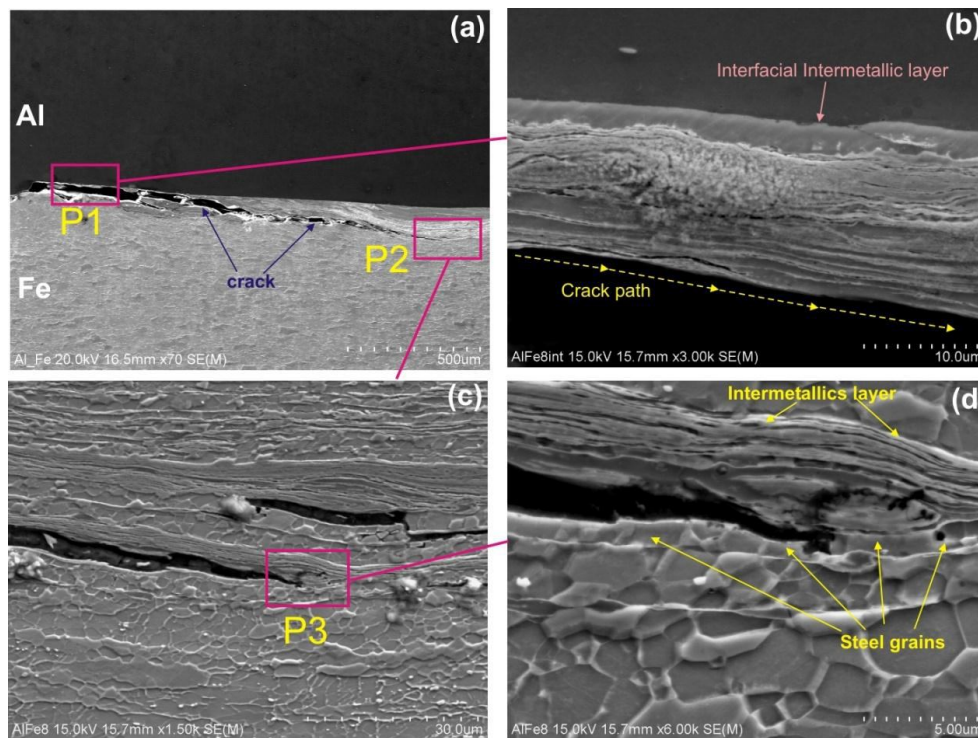


Fig. 12 Fractured path shown in SEM micrographs of a tensile-shear sample of welds stopped at $F_m/w_s = 265 \text{ N/mm}$ and unloaded.

As has been shown, F_m/w_s values of all pin-penetrating and defects-free welds in the present work and those from Movahedi et al. [18, 19] are largely the same or very close. Thus, it can be suggested that the manner of crack growth and the load required for the crack growth to failure are largely the same for all defects-free welds with a mixed stir zone. It should be noted that, as is indicative in Fig. 12(a), along the major crack there are some tiny bridges. The high magnification micrograph shows that the crack path is not very straight; rather there is an indication of a slightly torturous cracking path (Fig. 12b). This may also be consistent with the appearance of the SEM micrograph in Fig. 11b, indicating the fracturing path may have gone through one ‘hump’ to another. This is reasonable if the morphology of the mixed stir zone is considered. The thin intermetallic layers in the zone are not completely flat and a layer is not wide or lengthy due to the severe stir motion in the zone during friction stir. Spatially, the layers may take the shape of ‘hump’, laminated and filled with fine α -Fe grains in between. Thus, a crack propagating from a ‘hump’ to another needs to be fractured through some α -Fe material (bridges), which is comparatively tough. The crack tip propagated to α -Fe grain is evident in the high magnification micrograph in Fig. 12a & b. For this reason, a mixed stir zone is not completely a brittle zone and the fracture strength of the zone, $F_m/w_s \sim 310 \text{ N/mm}$, is not viewed low.

It should be noted that even in the advanced stage of cracking ($\sim 90\% F_m/w_s$) in the pin penetrating (Location2) sample, as has been presented and shown in Fig. 12c & d, little cracking has been observed along the interface intermetallic layer. On the other hand, when there is not a mixed stir zone, but the interface intermetallic layer has remained, as in Location 1 sample, fracture took place in the adjacent Al after a high amount of shear deformation as indicated by the SEM micrograph in Fig. 11a and the tensile shear curve in Fig. 9. Thus, it can be suggested that the presence of an interface intermetallic layer, which as has already been explained does not grow beyond $3\mu\text{m}$ and which is the condition for a continued metallurgical bonding, is actually a condition for high weld strength. A further condition of a high strength weld is the absence of a mixed stir zone due to the fact that cracks can propagate readily along the thin intermetallic layers in this zone under a significantly lower load.

4. Conclusions

For FSLW of aluminum alloy to steel (Al-steel), a little pin penetration to steel can result in a reasonable good joint strength (F_m/w_s), but this condition does not represent the optimal condition. Under a tensile-shear load, cracks propagate along the thin and discontinuous intermetallic layers inside the mixed stir zone resulting in a brittle fracture although cracks also need to propagate through the bridging α -Fe grains in the zone. The required F_m/w_s ($\sim 307 \text{ N/mm}$) for this fracture mode were not significantly affected by the size of the zone and by the coarseness of the microstructures in the zone. Thus, under the slight pin penetrating condition, F_m/w_s were not significantly affected by



penetration depth (D_p), rotation speed and forward speed. As D_p reaches to zero, a thin and continuous interface intermetallic layer formed without the mixed stir zone. Evidences have suggested that this interface layer is high in shear fracture resistance that the adjacent aluminum deforms to fracture instead and F_m/w_s in turn have high (450 N/mm) which is highest for the defect free Al-steel FSLW, compared to all the previous research for the specific FSLW conditions. Microstructure evidences, temperature histories determined and consideration based on growth kinetics of Fe–Al interface intermetallic layer have suggested that an interface intermetallic layer can only remain thin and does not grow beyond $3\mu\text{m}$ during FSLW. On the other hand, if the pin is away from the bottom steel piece during FSLW, there would not be a sufficient coverage of intermetallic compounds from Al-steel reaction to form a continued interface intermetallic layer. Thus, joining becomes discontinued and F_m/w_s decreases.

References

- [1] Taban E, Gould JE, Lippold JC (2010) *Mater Des* 31:2305
- [2] Liedl G, Bielak R, Ivanova J, Enzinger N, Figner G, Bruckner J, Pasic H, Pudar M, Hampel S (2011) *Procedia* 12:150
- [3] H. T. Zhang, J. C. Feng, P. He, B. B. Zhang, J. M. Chen and L. Wang, *Mater. Sci. Eng., A* 499 (1-2), 111- 113 (2009)
- [4] G. Sierra, P. Peyre, F. Deschaux-Beaume, D. Stuart and G. Frasn, *Materials Science and Engineering: A* 447 (1–2), 197-208 (2007)
- [5] G. Sierra, P. Peyre, F. Deschaux-Beaume, D. Stuart and G. Frasn, *Mater. Charact.* 59 (12), 1705-1715 (2008).
- [6] C. Y. Choi, D. C. Kim, D. G. Nam, Y. D. Kim and Y. D. Park, *J Mater Sci Technol* 26 (9), 858-864 (2010).
- [7] L. A. Jácome, S. Weber, A. Leitner, E. Arenholz, J. Bruckner, H. Hackl and A. R. Pyzalla, *Adv. Eng. Mater.* 11 (5), 350-358 (2009).
- [8] H. Springer, A. Kostka, E. J. Payton, D. Raabe, A. Kaysser-Pyzalla and G. Eggeler, *Acta Mater.* 59 (4), 1586-1600 (2011).
- [9] L. Agudo, D. Eyidi, C. H. Schmaranzer, E. Arenholz, N. Jank, J. Bruckner and A. R. Pyzalla, *J Mater Sci* 42 (12), 4205-4214 (2007)
- [10] R. S. Coelho, A. Kostka, J. F. dos Santos and A. Kaysser-Pyzalla, *Mater. Sci. Eng., A* 556, 175-183 (2012)
- [11] Ozdemir, N.; Sarsilmaz, F.; Hascalik, A. Effect of Rotational speed on the interface Properties of friction welded AISI 304L to 4340 to steel. *Mater. Des.* 2007, 28, 301–307.
- [12] Dehghani, M.; Amadeh, A.; AkbariMousavi, S.A.A. Investigations on the effects of friction stir welding parameters on intermetallic and defect formation in joining aluminum alloy to mild steel. *Mater. Des.* 2013, 49, 433–441.
- [13] Watanabe, T.; Takayama, H.; Yanagisawa, A. Joining of aluminum alloy to steel by friction stir welding. *J. Mater. Process. Technol.* 2006, 178, 342–349.
- [14] Elrefaey A, Gouda M, Takahashi M, Ikeuchi K (2005) *J Mater Eng Perform* 2005(14):10
- [15] Kimpapong K, Watanabe T (2005) *Mater Trans* 46:835
- [16] Kimpapong K, Watanabe T (2005) *Mater Trans* 46:2211
- [17] Coelho RS, Kostka A, Sheikhi S, dos Santos JF, Pyzalla AR (2008) *AdvEng Mater* 10:961
- [18] Movahedi M, Kokabi AH, SeyedReihani SM, Najafi H (2011) *ProcediaEng* 10:329
- [19] Movahedi M, Kokabi AH, SeyedReihani SM, Najafi H (2012) *SciTechnol Weld Join* 17:162
- [20] Xiong JT, Li JL, Qian JW, Zhang FS, Huang WD (2012) *SciTechnol Weld Join* 2012(17):196
- [21] Y. Wei, J. Li, J. Xiong and F. Zhang, *J. Mater. Eng. Perform.* 22 (10), 3005-3013 (2013).
- [22] Y. C. Chen and K. Nakata, *Metall. Mater. Trans. A* 39 (8), 1985-1992 (2008).
- [23] Zheng, Q.; Feng, X.; Shen, Y.; Huang, G.; Zhao, P. Dissimilar Friction stir welding of 6061 Al to 316 stainless steel using Zn as a Filler Metal. *J. Alloys Compd.* 2016, 686, 693–701.
- [24] Naoi D, Kajihara M (2007) *Mater SciEng A* 459:375
- [25] Springer H, Kostka A, dos Santos JF, Raabe D (2011) *Mater SciEng A* 528:4630